

Received: 2018.07.27
Accepted: 2018.08.27
Published: 2018.09.19

Protective Effects of Oleuropein Against Cerebral Ischemia/Reperfusion by Inhibiting Neuronal Apoptosis

Authors' Contribution:
Study Design A
Data Collection B
Statistical Analysis C
Data Interpretation D
Manuscript Preparation E
Literature Search F
Funds Collection G

ACDF 1 **Weijing Zhang**
ABE 2 **Xiaogang Liu**
DF 1 **Qiuyue Li**

1 Department of Nursing, Tangshan Gongren Hospital, Tangshan, Hebei, P.R. China
2 Department of Hepatobiliary Surgery, Tangshan Gongren Hospital, Tangshan, Hebei, P.R. China

Corresponding Author: Xiaogang Liu, e-mail: chensits@163.com
Source of support: Departmental sources

Background: In this study, we investigated the potential neuroprotective effect of oleuropein (OLE) on apoptotic changes via modulating Akt/glycogen synthase kinase 3 beta (Akt/GSK-3 β) signaling in a rat model of cerebral ischemia/reperfusion injury (IRI).

Material/Methods: Sprague-Dawley male rats (12 weeks, n=200) were randomly assigned to 5 groups: sham group, vehicle (IRI+vehicle) group, OLE (IRI+OLE) group, OLE+LY294002 (IRI+OLE+LY294002) group, and LY294002(IRI+LY294002) group. The rats were subjected to cerebral ischemia/reperfusion injury (IRI) model and treated once daily for 5 days with vehicle and OLE (100 mg/kg via intraperitoneal injection) after IRI injury. LY294002 (0.3 mg/kg) was intraperitoneally injected once at 30 min after IRI injury. Brain edema, neurological deficit, rotarod latencies, and Morris water maze (MWM) performance were evaluated after IRI. The number of dead cells were assayed by TUNEL staining. Western blot was used to detect the expression of Bcl-2, Bax, cleaved caspase-3 (CC3), neurotrophic factors, and the phosphorylation levels of Akt and GSK-3 β .

Results: Compared with the vehicle group, brain water content, neurological deficits, rotarod latencies, and escape latency following IRI were reduced in the OLE group. Cell apoptosis and reduced neurotrophic factor caused by IRI was also attenuated by OLE. Furthermore, increased p-Akt and decreased p-GSK-3 β were caused by OLE, which were associated with decrease of Bax/Bcl-2 ratio and the suppression of Caspase-3 activity after IRI. Importantly, all the beneficial effects of OLE in the vehicle group were abrogated by PI3K inhibitor LY294002.

Conclusions: Cerebral ischemia was protected by OLE via suppressing apoptosis through the Akt/GSK-3 β pathway and up-regulating neurotrophic factor after IRI.

MeSH Keywords: **Apoptosis • Brain Ischemia • Olea • Phosphatidylinositol 3-Kinases • Proto-Oncogene Proteins c-akt**

Full-text PDF: <https://www.medscimonit.com/abstract/index/idArt/912336>

 4035  —  7  50



Background

Cerebral ischemia (CI) is one of the leading causes of death and the most frequent cause of permanent disability in adults worldwide. The poor outcomes of CI are usually attributable to the detrimental effects of acute cerebral ischemia-reperfusion injury [1–3]. Although accounting for approximately 3–7% of the total health-care expenditure used in high-income countries, cerebral ischemia still remains the most frequent cause of permanent disability, and the second most common cause of dementia [4]. Ischemia/reperfusion injury (IRI) refers to the cerebral lesion caused by blood supplication after a period of ischemia [5]. The pathogenesis of IRI involves a complex sequence of physiological events, including documented inflammatory cascade, excitotoxicity, oxidative stress, deficiencies in nerve growth factor, and presence of apoptosis [6–8]. Accumulating evidence suggests that neuronal apoptosis represents a prominent form of cell death which leads to declines in neurological functions during IRI [9,10]. Because intact neurons are the basis of normal nerve function, inhibition of neuronal apoptosis contributes to the recovery of neurological function and effectively improves the long-term prognosis of patients.

Oleuropein (OLE) is a natural secoiridoid that is isolated from the plant *Olea europaea*, which is involved in the course of physiological and pathological processes in a wide range of diseases [11,12]. OLE has long been reported to exhibit several pharmacological activities after central nervous system disease such as Alzheimer's disease (AD), traumatic brain injury, and stroke [13]. In addition, oleuropein has been shown to exert a protective effect against ischemia/reperfusion-induced cardiomyopathy via anti-inflammatory and anti-hypoxia reoxygenation [14]. In the context of ischemia-reperfusion injury, OLE can reduce cellular apoptosis via the activation the phosphatidylinositol 3-kinase (PI3K)-Akt and extracellular signal-regulated kinase 1/2 (ERK1/2) signaling pathway kinase in ischemic myocardial injury [15]. OLE was also proved to provide neuroprotection by suppressing neuronal cell death in rats with spinal cord injury [16]. However, whether the effect of OLE administration on the apoptotic response is associated with recovery of neurological function during IRI and the potential mechanisms underlying these effects has been unclear.

The Akt/Glycogen synthase kinase 3 β (Akt/GSK-3 β) signaling pathway is critically involved in cell proliferation and apoptosis in many cell types, including hippocampal neurons [17,18]. The repressed Akt and stimulated GSK-3 β have been proved to exacerbate neuronal damage in experimental intracerebral hemorrhage and diabetic encephalopathy [19,20]. There is compelling evidence that the PI3K-Akt pathway is the upstream signal pathway that negatively regulates the expression of GSK-3 β [21,22]. Further studies of OLE and its potential anti-apoptotic mechanisms may provide evidence that

OLE is a candidate therapeutic target to reduce neuron apoptosis and promote neurological functional recovery after IRI. In the present study, we attempted to clarify the role of OLE in amelioration of neurological and cognitive outcomes by inhibiting apoptosis in a rat model of IRI. The Akt/GSK-3 β pathway was hypothesized and detected as a possible positive mechanism of OLE effects.

Material and Methods

Animals

Adult male Sprague-Dawley (SD) rats (12 weeks old, weighing 230–260 g) were obtained from Vital River Laboratories, Beijing, China (Certificate No: SCXK2016-0006) and were used for these experiments. The procedures for this study were approved by Animal Care and Use Committee of North China University of Science and Technology and were carried out in accordance with the Guide for the Chinese Council on Animal Protection. All rats were allowed free access to food and water under controlled conditions (12/12 h light/dark with humidity 50–60% and temperature 22–24°C).

IRI model

To establish a transient acute cerebral infarction model, rats underwent right middle cerebral artery occlusion (MCAO) surgery according to the intraluminal suture method previously described by Longa et al. [23]. Rats were fasted for 8 h before surgery and following anesthetization with 10% chloral hydrate (350 mg/kg) intraperitoneally. The rats were placed in a supine position with body temperature maintained at 36.5–37.5°C. A Laser-Doppler flowmeter (moor-VMSLDF, Moor Instruments, Ltd, UK) was utilized to monitor regional cerebral blood flow (rCBF). The bilateral common carotid artery (CCA), external carotid artery (ECA), and internal carotid artery (ICA) was exposed via mid-neck incision. After closing the right CCA with a microclip, monofilament nylon suture was inserted from the CCA into the lumen of the ICA to block the origin of the middle cerebral artery (MCA). Performance of the MCAO surgery was regarded as successful if rCBF was reduced abruptly by 80–90%. The occlusion of the MCA through the intraluminal suture was maintained for 60 min, followed by removal and reperfusion. The sham group had the same surgical procedures without inserting a filament. In the course of the establishment of the experimental group in the IRI model, a total of 12 rats died.

Experimental groups and treatment

We randomly assigned 200 adult rats to 5 groups (n=40): the sham group, the vehicle (IRI+vehicle) group, the OLE

(IRI+OLE) group, OLE+LY294002 (IRI+OLE+LY294002) groups, and the LY294002 (IRI+LY294002) group. SD rats in the vehicle group, OLE group, OLE+LY294002 group, and LY294002 group were subjected to IRI surgery. Oleuropein (Sigma Aldrich, Germany) was dissolved in physiological saline which included 3% dimethyl sulfoxide (DMSO). Rats were administered oleuropein at 30 min after IRI surgery at a dose of 100 mg/kg via intraperitoneal injection and then received it once a day for 5 days. The PI3K inhibitor LY294002 (0.3mg/kg; Cell Signaling Technology, Inc., Beverly, MA, USA) was solubilized in physiological saline which included 3% DMSO and intraperitoneal injected at 30 min after the induction of IRI. In the sham and vehicle groups, an equal volume of physiological saline including DMSO was administered in the same manner. The rats were allowed to recover spontaneous ventilation.

Neurological score

Neurological deficit of the rats was evaluated by modified neurological severity score (mNSS), which is a composite of motor tests, sensory tests, beam balance tests, and reflexes absent [24]. In the present study, it used to grade various aspects of neurobehavioral function on days 1–5 after IRI. The lower the score, the better the function (normal score=0, maximal deficit score=18).

Rotarod test

In addition to the mNSS score, the rats were evaluated on the basis of an accelerating automated rotarod, which was used to measure the effects of therapeutic intervention on vestibulomotor function [25]. In order to obtain baseline values, the rats were tested before IRI was induced. Tests were performed on days 1–5 after IRI to assess early motor outcome. As the speed increased from 4 to 40 rpm within 5 min, average time elapsed from the rotation of the cylinder was recorded. If the rats dropped twice from the device, the experiment ended.

Morris water maze test

Spatial learning and memory were assessed using the Morris water maze at 1–5 days following IRI. Before the navigation task, the rats were allowed to swim for 5 min in a circular water tank (180 cm in diameter and 45 cm in depth) divided into 4 equivalent quadrants: north (N), west (W), south (S), and east (E). They were trained to find a submerged escape platform (14 cm in diameter), which was located in the middle of one of the quadrants equidistant from the sidewall at a fixed time each day. Rats were allowed a maximum of 120 s to find the platform prior to IRI or sham operation. The rats were placed randomly in the water facing the wall of the tank. If the rats successfully found the platform during the Morris water maze test, they would be left on the platform for 15 s prior

to the start of the next training section. On day 5 of the spatial tests, the platform was removed and the rats were placed into the water at the same randomly selected starting points. Maze performance was recorded using a video camera located above the pool and interfaced with a video tracking system (HVS Imaging, Hampton, UK). The mean escape latency of a total of the previous 4 trials and the times spent in the target quadrant on day 5 were then calculated.

Brain water content

The rats were anesthetized and euthanized on days 1–3 after IRI. Brain water content was measured using the standard wet-dry method, which has been widely used [26]. After brains were sectioned in the mid-sagittal plane, the hemispheres were weighed immediately to obtain wet weight. Then, the hemispheres were dried at 90°C for 24 h to obtain the dry weight. We calculated water content as a percentage of wet weight ($[(\text{wet weight} - \text{dry weight}) / \text{wet weight}] \times 100$).

Cell death analysis by terminal deoxynucleotidyl transferase-mediated (dUTP) nick-end Labeling (TUNEL) staining

The cell death of neurons was detected by TUNEL staining as described previously [27]. Briefly, after behavioral tests, the rats that were anesthetized with chloral hydrate and sacrificed via transcardiac perfusion with cold phosphate-buffered saline (PBS), followed by 4% paraformaldehyde in 0.1 M phosphate buffer, to pre-fix the brain tissue. Brain tissue specimens from the cerebral ischemia area were embedded in paraffin and then cut into serial sections at a thickness of 5 μm using a microtome. Following deparaffinization and rehydration, the paraffin sections were rinsed twice in 0.1 M PBS and incubated with Proteinase K working solution (10 $\mu\text{g}/\text{ml}$ in 10 mM Tris/HCl, pH 7.5–8.0) for 15 min at 37°C. The sections were washed in PBS again, then treated with green fluorescein-labeled dUTP solution containing 10% TdT. Finally, the paraffin sections were counterstained with DAPI. TUNEL-positive cells exhibiting green fluorescent granules were determined using a fluorescence microscopy (Olympus, Japan) and were quantified by counting 5 randomly selected microscopic fields.

Western blot analysis

Following behavioral tests on day 5, the rats were sacrificed by an overdose of chloral hydrate. The brain tissue of each rat was excised and flash-frozen in liquid nitrogen until use. In order to detect protein expression adequately, an appropriate amount of frozen brain samples was minced with eye scissors in ice. Then, the tissue was homogenized in cold Tissue Protein Lysis Solution (Thermo Fisher Scientific, Inc., Waltham, MA, USA) and clarified by centrifuging

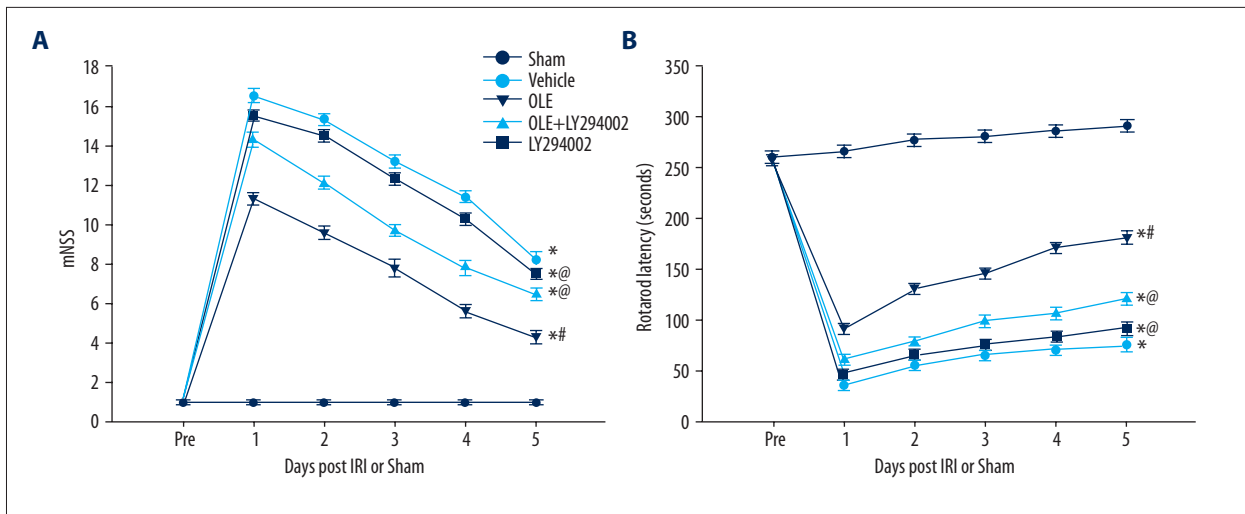


Figure 1. Based on neurobehavioral function and rotarod motor test, neurological function showed considerable improvement in OLE-treated rats over 5 days following IRI. The OLE treatment significantly decreased the mNSS scores compared with the vehicle group at 1–5 days after IRI (A). The vestibulomotor performance by rotarod testing was also significantly improved in the OLE group at 1–5 days after IRI (B). Data are presented as the mean \pm SEM (* $P < 0.05$ compared with sham, # $P < 0.05$ compared with vehicle, @ $P < 0.05$ compared with OLE, $n = 8$ –10/group).

(12 000 \times g for 20 min at 4°C) before taking the supernatant. Protein concentration was determined using the BCA reagent (ZSGB-Bio, Beijing, China) method. A total of 25 μ g of extracted protein were subjected to SDS-polyacrylamide gel electrophoresis and transferred onto a polyvinylidene difluoride membrane (PVDF). After blocking with 5% fat-free dry milk for 2 h at room temperature, the membrane was then incubated overnight at 4°C with primary antibody, including Akt (anti-rabbit, 1: 1000, Abcam), p-Akt (anti-rabbit, 1: 1000, Abcam), GSK3 β (anti-rabbit, 1: 1000, Abcam), p-GSK3 β (anti-rabbit, 1: 1000, Abcam), β -actin (anti-rabbit, 1: 1000, Abcam), cleaved caspase-3 (CC3, anti-mouse, 1: 1000; Cell Signaling), caspase-3 (anti-rabbit, 1: 1000, Abcam), B-cell leukemia/lymphoma 2 (Bcl-2, anti-rabbit, 1: 1000, Abcam), BCL2-Associated X (Bax, anti-rabbit, 1: 1000, Abcam), brain-derived neurotrophic factor (BDNF; anti-rabbit, 1: 1000, Abcam), and nerve growth factor (NGF; anti-rabbit, 1: 1000, Abcam). Nitrocellulose membranes were then labeled with secondary antibodies for 1 h at 4°C. Bands were visualized by using an enhanced chemiluminescent (Bio-Rad, Hercules, CA, USA) reagent and were analyzed by ImageJ 1.41 software (National Institutes of Health, Bethesda, MD, USA).

Detection of Caspase-3 activity

Caspase-3 activity was determined using the tissue caspase-3 colorimetric activity assay kit purchased from Genmed Scientific, Inc. (Shanghai, China). The brain tissues, which were grounded in liquid nitrogen, were homogenized with chilled tissue lysis buffer, incubated on ice for 10 min, and centrifuged for 5 min in a microcentrifuge (12 000 \times g). The supernatant was collected into a tube and the samples were read in a microtiter

plate reader. The absorbance of each well was measured at 405 nm with a microtiter plate reader. Comparison of the OD from induced apoptotic samples with an un-induced control allowed determination of the fold-increase in caspase-3 activity.

Statistical analyses

All data are presented as the mean \pm standard deviation and were analyzed using SPSS 21.0. Each experiment was repeated a minimum of 3 times. The data were analyzed by one-way ANOVA, followed by Bonferroni post hoc test for multiple comparisons. $P < 0.05$ was considered to indicate a statistically significant difference.

Results

OLE attenuated neurofunctional deficits.

The mNSS scores and rotarod testing are a comprehensive evaluation of neurological functions in rats, while the MWM test reflects spatial learning and memory ability. As presented in Figure 1A, IRI induced a significant neurological deficit in the vehicle group as compared with the sham group over 5 days after IRI ($P < 0.05$), whereas the administration of OLE significantly reduced the mNSS scores when compared with the vehicle group ($P < 0.05$). When OLE was combined with the PI3K inhibitor LY294002 (OLE+LY294002), mNSS scores were higher than in the OLE group ($P < 0.05$). LY294002 did not increase mNSS when administered alone compared with the vehicle group ($P > 0.05$). There was no statistically significant difference in mNSS scores

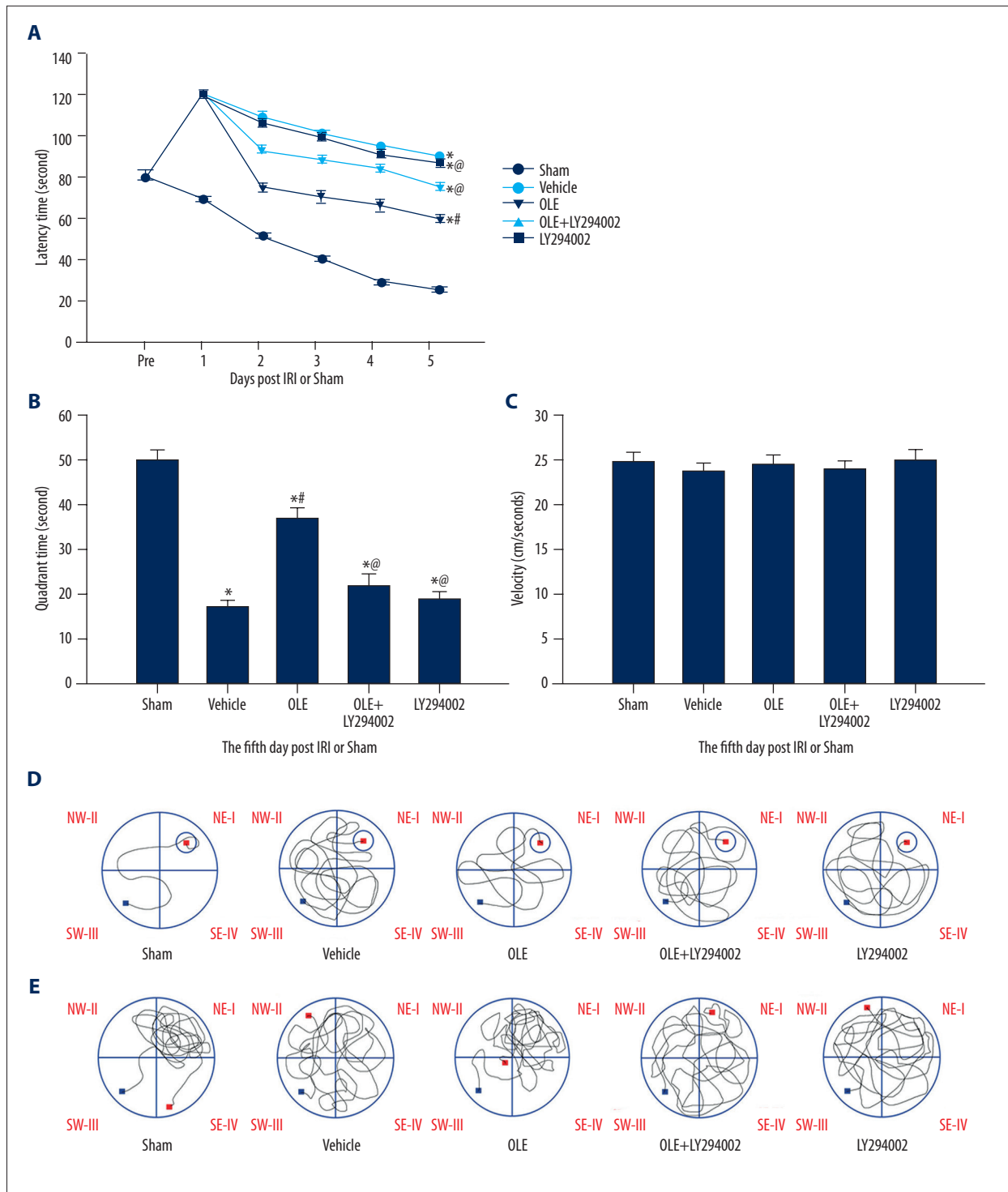


Figure 2. Cognitive function showed improvement in OLE rats over 5 days following IRI based on MWM test. The OLE treatment significantly improved learning and memory capability compared with the vehicle group over 5 days after IRI. The spatial learning performance by orientation navigation experiments testing also showed clear improvement in the OLE group over 5 days after IRI (A). Time spent in the target quadrant following removal of the platform was reduced by OLE treatment (B). There were no significant differences in swim speeds among groups (C). Representative traces indicating the sample paths of the rats from the maze latency trials (D) and the probe trials (E) on day 5. Data are presented as the mean \pm SEM (* $P < 0.05$ compared with sham, # $P < 0.05$ compared with vehicle, @ $P < 0.05$ compared with OLE group, $n = 8-10$ /group).

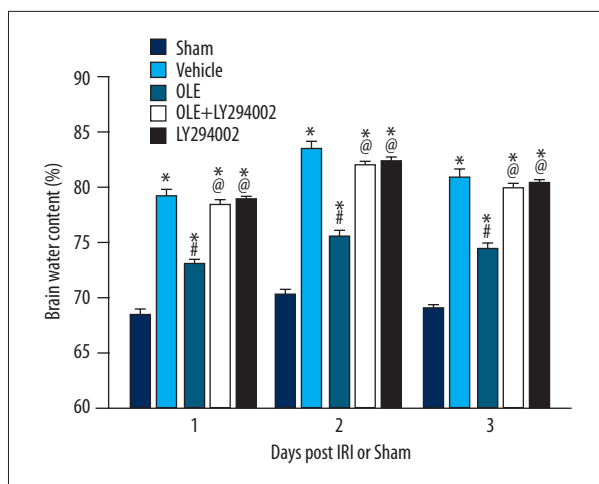


Figure 3. Brain water content was reduced in OLE rats on days 1–3 after IRI. Data in bar graphs are presented as mean \pm SEM. (* $P < 0.05$ compared with sham, # $P < 0.05$ compared with vehicle, @ $P < 0.05$ compared with OLE, $n = 6-8$ /group).

between vehicle group and OLE+LY294002 group ($P > 0.05$). The rotarod latencies of OLE-treated rats were significantly longer than that of vehicle-treated rats (Figure 1B, $P < 0.05$), whereas OLE+LY294002 group rats lagged behind the OLE group. There was a significant difference in rotarod latencies between the OLE group and OLE+LY294002 group ($P < 0.05$). LY294002 did not induce a significant decrease of rotarod latencies when administered alone compared with the vehicle group ($P > 0.05$).

OLE ameliorated cognitive deficits

As presented in Figure 2A, the sham-operated rats did not have any spatial learning or memory deficits. Statistical analysis confirmed that the vehicle group had significantly longer escape latency than in the sham group over 5 days after reperfusion ($P < 0.05$). There was a significant decrease in escape latency of the OLE group compared to the vehicle group ($P < 0.05$). OLE+LY294002 increased the escape latency of rats compared with the OLE group ($P < 0.05$). Although LY294002 alone reduced the escape latency slightly, no statistically significant difference was observed between the vehicle group and LY294002 group ($P > 0.05$). Following 4 days of testing, the platform was removed. Under these conditions, the time spent in the target quadrant was significantly lower for the vehicle group than for the sham group, but was significantly increased in the OLE treatment group compared with the vehicle group (Figure 2B). Compared with the OLE group, OLE+LY294002 deteriorated impairments to spatial learning and memory by shortening the time spent in the target quadrant. However, there was no significant effect in the LY294002 group compared with the vehicle group ($P > 0.05$). Nevertheless, there were no significant differences in swim speeds among groups (Figure 2C).

OLE alleviated brain edema

The brain water content in the ischemic hemisphere was analyzed on days 1–3 after IRI induction. There was a significant increase in brain water content in the vehicle group compared to the sham group ($P < 0.05$, Figure 3). OLE significantly decreased brain edema content compared to the vehicle group ($P < 0.05$). Nevertheless, the rats receiving OLE combined with LY294002 did not have reduce brain edema content compared to the OLE group ($P < 0.05$). LY294002 did not increase brain edema when administered alone compared with the vehicle group ($P > 0.05$).

OLE administration prevents neuronal cell loss at day 5 after IRI

TUNEL/DAPI staining was performed to clarify the role of OLE in cell death, which revealed a high density of positively stained cells within the infarct area itself as well as in the surrounding periphery. DAPI was used for nuclear staining. Cells co-stained with TUNEL and NeuN were deemed as neuronal death (Figure 4A). The results of quantitative analysis showed significant differences between the groups in ischemic regional TUNEL-positive cell ($P < 0.05$, Figure 4B). In the sham group, few TUNEL-positive dead cells were found. The cell loss index in the ischemic region of the vehicle group was significantly increased compared with those in the sham group ($P < 0.05$, Figure 4A). In comparison with the vehicle group, the administration of OLE significantly reduced TUNEL-positive cells ($P < 0.05$). However, after administration of OLE+LY294002, the number of TUNEL-positive cells was significantly increased compared with the OLE group ($P < 0.05$).

OLE decreased the ratio of Bax/Bcl-2 and downregulated CC3 expression and Caspase-3 activity after IRI

Western blotting was used to detect CC-3, Bax, and Bcl-2 protein levels in the ischemic hemisphere. By comparison with the sham group, it revealed a remarkable increase in the ratio of Bax/Bcl-2 in the vehicle group ($P < 0.05$, Figure 5A). IRI-induced increases in the Bax/Bcl-2 ratios were attenuated by treatment with OLE ($P < 0.05$), while this protection was hindered by LY294002 (OLE+LY294002) administration ($P < 0.05$, Figure 5A). CC3 is another important marker of apoptosis detected in the present study. As presented in Figure 5B, the level of CC3 in the rat's cerebellums differed considerably among the groups in our present study. Compared with the sham group, cerebral CC3 was significantly increased in the vehicle group and significantly downregulated by OLE treatment compared with the vehicle group, whereas treatment with LY294002 combined with OLE evidently increased the expression of CC3 compared with OLE after reperfusion ($P < 0.05$, Figure 5B). Similarly, OLE reduced IRI-induced increased caspase-3 activity, while it was impeded by LY294002 (OLE+LY294002) administration

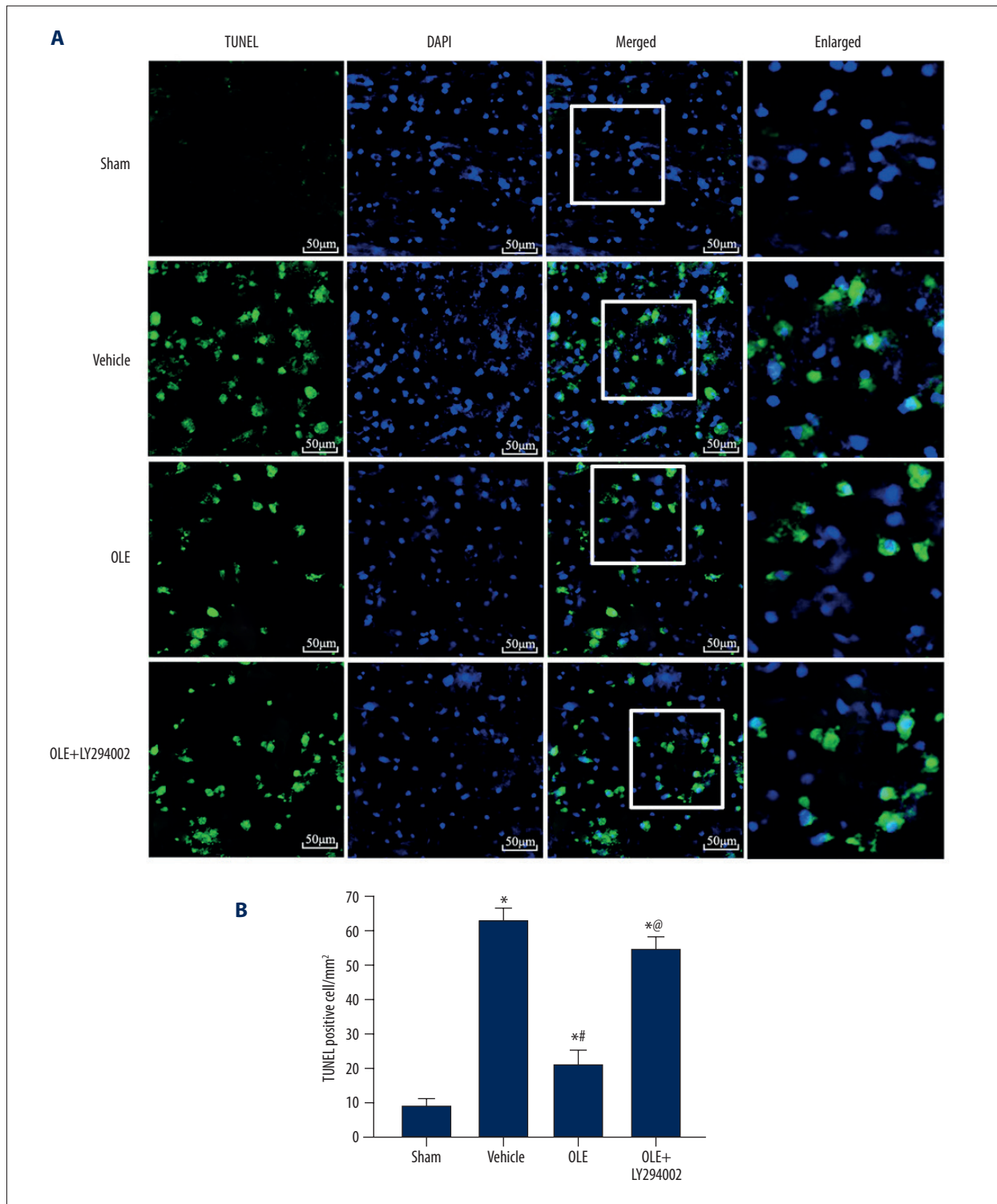


Figure 4. Co-staining of TUNEL (green) and DAPI (blue) in the perihematomal cerebral cortex at day 5 after IRI. TUNEL-positive cells were barely detected in the sham group but were widely distributed in the ischemic region after IRI. OLE decreased the number of TUNEL-positive cells, which was blocked by LY294002. Scale bar 50 μ m (**A**). IRI increased the number of TUNEL-positive cells compared with the sham group, whereas OLE clearly reduced the number of TUNEL-positive cells. Moreover, LY294002 combined with OLE reversed the declining trend compared with OLE only treatment (**B**). Data are presented as the mean \pm SEM (* $P < 0.05$ compared with sham, # $P < 0.05$ compared with vehicle, @ $P < 0.05$ compared with OLE, $n = 6-8$ /group).

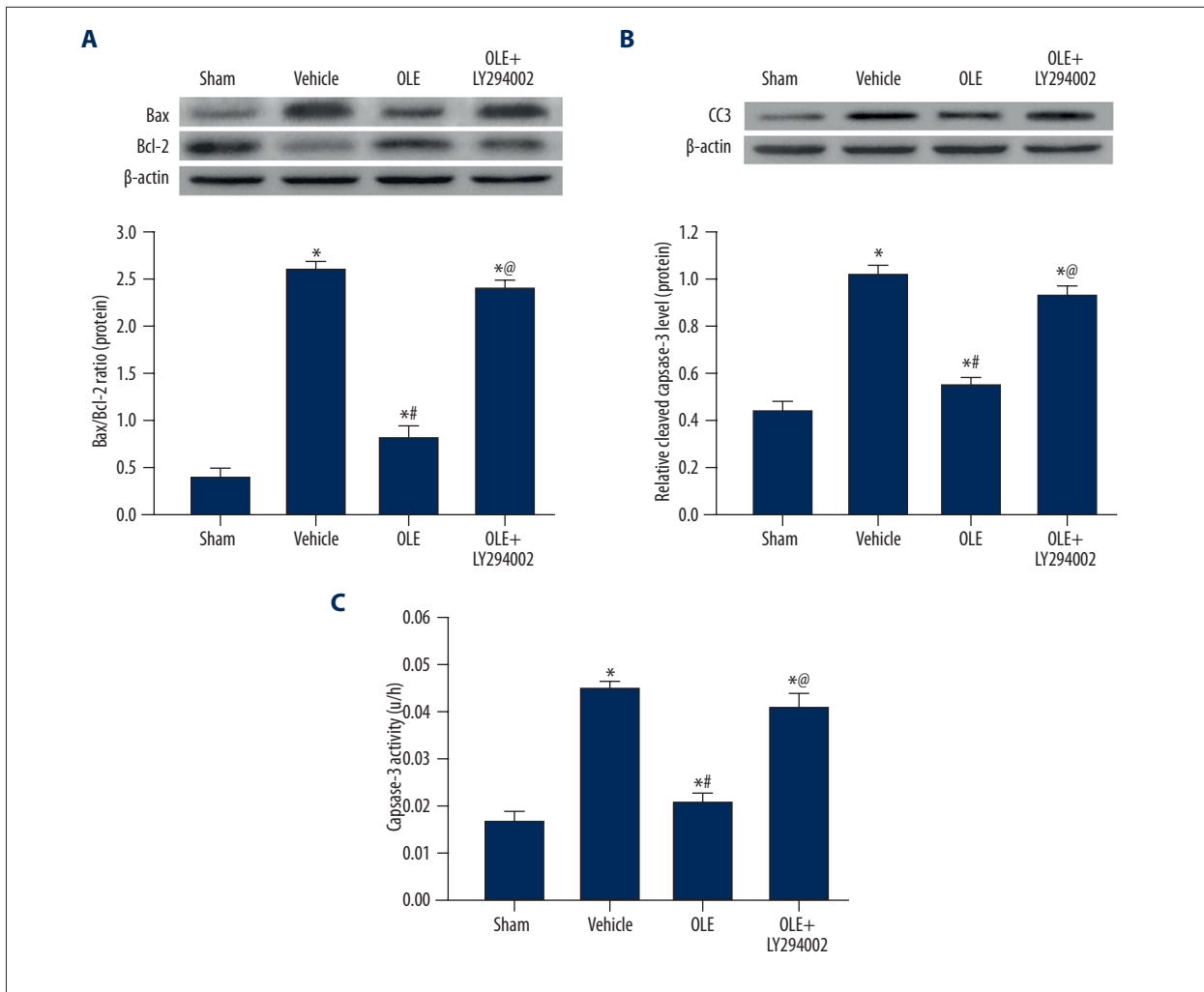


Figure 5. OLE affects Bcl-2 family, cleaved caspase-3 protein expression, and Caspase-3 activity on day 5 after IRI or sham. Representative Western blots and densitometric quantification of Bax/Bcl-2 (**A**). Representative Western blots and densitometric quantification and cleaved caspase-3/ β -actin on day 5 after IRI (**B**). Caspase-3 activity in brain tissues of rats in different groups (**C**). Data are presented as the mean \pm SEM (* $P < 0.05$ compared with sham, # $P < 0.05$ compared with vehicle, @ $P < 0.05$ compared with OLE, $n = 8-10$ /group).

($P < 0.05$, Figure 5C). However, there was no significant difference in Bax/Bcl-2 ratio and CC3 or caspase-3 activity between the vehicle group and the OLE+LY294002 group ($P > 0.05$).

OLE activated the Akt/GSK-3 β signaling pathway after IRI

The Akt/GSK3 β pathway, which is activated by the phosphorylation at Ser473 via the PI3K pathway, has been proposed to serve a vital role in cell survival and to inhibit apoptosis [28]. As presented in Figure 6, the vehicle group exhibited significantly decreased p-Akt expression and significantly increased p-GSK3 β expression. OLE administration dramatically increased p-Akt expression and decreased p-GSK3 β expression compared with the vehicle group ($P < 0.05$, Figure 6), and this expression was reversed by OLE+LY294002 administration

($P < 0.05$, Figure 6). Treatment with OLE+LY294002 remarkably reduced the levels of p-Akt and increased p-GSK-3 β when compared with OLE alone. Nevertheless, there was no significant difference in p-Akt and p-GSK-3 β between the vehicle group and OLE+LY294002 group ($P > 0.05$). The expressions of total Akt and total GSK-3 β were constant in the sham and experimental groups ($P > 0.05$).

OLE reverses the decrease in neurotrophic factor expression after IRI

The expression of BDNF and NGF, which were both neurotrophic factors, decreased after IRI compared with the sham group in Western blot analysis ($P < 0.05$, Figure 7). In contrast, OLE administration dramatically restored IRI-induced decreases

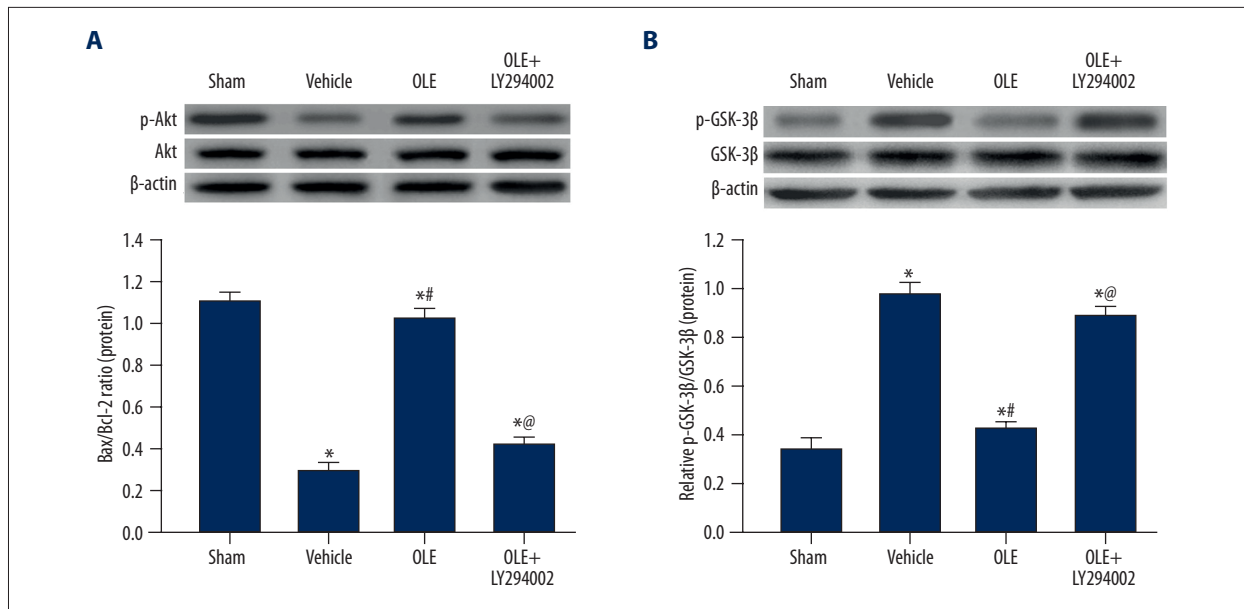


Figure 6. OLE affected p-Akt and p-GSK-3 β protein expression on day 5 after IRI or sham. Representative Western blots and densitometric quantification of p-Akt/total Akt (**A**). Representative Western blots and densitometric quantification of p-GSK3 β /total GSK3 β (**B**). Data are presented as the mean \pm SEM (* P <0.05 compared with sham, # P <0.05 compared with vehicle, @ P <0.05 compared with OLE, n=8–10/group).

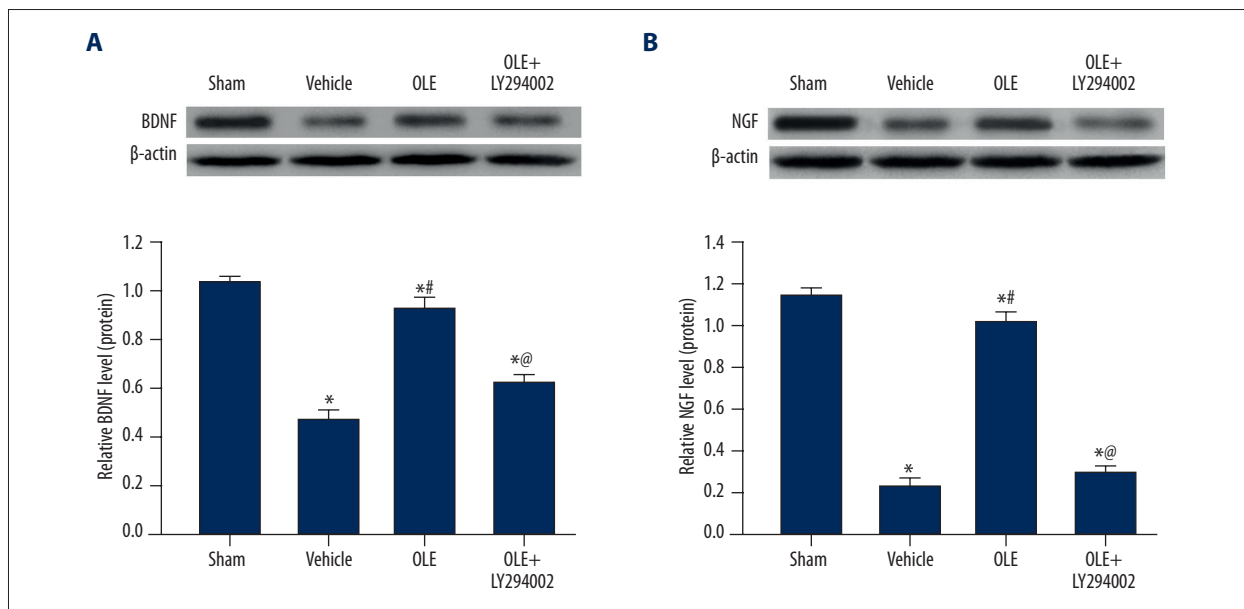


Figure 7. Administration of OLE affected BDNF and NGF protein expression on day 5 after IRI or sham. Representative Western blots and densitometric quantification of BDNF/ β -actin (**A**). Representative Western blots and densitometric quantification of and NGF/ β -actin on day 5 after IRI (**B**). Data are presented as the mean \pm SEM (* P <0.05 compared with sham, # P <0.05 compared with vehicle, @ P <0.05 compared with OLE, n=8–10/group).

in expression of BDNF and NGF, while this protection was hindered by OLE+LY294002 administration (P <0.05). OLE+LY294002 did not increase neurotrophic factors compared with the vehicle group (P >0.05).

Discussion

In the present study, OLE improved neurological and cognitive outcomes, alleviated brain edema, increased neurotrophic factors, and reduced apoptosis of neural cells by regulating

Akt/GSK-3 β signaling pathways in a classical experimental model rat model of IRI. Ischemic stroke is a neural and vascular disease caused by deprivation of blood flow when intracranial arteries are occluded. Ischemic stroke has gradually been identified to result from a surge in the activation of complex pathophysiological pathways, from ischemic injury initiation to secondary reperfusion injury [29,30]. Besides oxidative and nitrosative stress and inflammatory mechanisms, neuronal apoptosis equally predominates at the core of cerebral ischemic damage [8,31] and this has led researchers to explore intervention measures to improve the neurological and cognitive functions destroyed by cerebral ischemia in human patients. OLE is the main phenolic secoiridoid, which is extracted from olive trees, and is capable of producing antioxidant, anti-apoptotic, antimicrobial, anti-inflammatory, and neuroprotective activity [32–34]. Increasing evidence suggests that OLE can help cells with normal functions survive in a variety of adverse situations such as ischemic diseases involving the brain and other organs [35,36]. A previous study demonstrated that OLE displayed an anti-apoptosis response via anti-inflammatory actions, as well as suppression of lipid peroxidation and neutrophil infiltration in a mouse model of spinal cord trauma [37]. Moreover, oral administration of OLE ameliorates cerebral injury in a rat model of IRI by inhibiting the expression of apoptosis-related Bax, thereby suppressing Bcl-2 activation [38]. Nevertheless, the underlying mechanisms of OLE in apoptosis associated with neurological recovery in IRI still remains poorly elucidated. In the present study, OLE alleviated IRI-induced cerebral edema and improved neurological and cognitive function outcomes of mNSS scores, rotarod test, and MWM test on days 1–5 after IRI induction. OLE also significantly attenuated apoptosis in neuronal cells. Therefore, we investigated whether the neuroprotective effects of OLE were regulated by inhibiting the apoptosis-related Akt/GSK-3 β signaling pathway. Rats receiving OLE administration had neuroprotective effects compared with the vehicle group. Treatment with OLE combined with LY294002 increased the number of apoptotic cells, which abolished the anti-apoptosis effect of OLE alone. Our findings further confirm results of a previous study that reported administration of LY294002 alone did not provoke neuron apoptosis compared with the vehicle group after IRI [39]. Our findings show that OLE exert their neuroprotective effects through the Akt/GSK-3 β signaling pathway.

Apoptosis, which is executed by proteases called caspases, is of importance for tissue homeostasis [40]. Bcl-2 family proteins are apoptosis-related proteins serving as central regulators of caspase activation. The BCL-2 family members include both pro- and anti-apoptotic molecules. Bcl-2 acts as anti-apoptotic factor, while Bax promotes apoptosis [41]. Indeed, the ratio of Bax and Bcl-2 helps to determine the extent of apoptosis. CC3 is another key executor involved in cell apoptosis [42]. In our present study, the imbalanced expression

of Bax/Bcl-2 and increased CC3 expression resulted from cerebral ischemic-reperfusion injury, while treatment OLE for 5 days resulted in a reduction of Bax/Bcl-2 ratio and CC3 expression. Consistent with the present study, Yu et al. [43] also proposed the anti-apoptosis effect of OLE on the regulation of BCL-2 family members in IRI. The same phenomenon occurred in the TUNEL staining assay. There was an obviously reduced density of TUNEL-positive cells in the OLE treatment group, suggesting that OLE suppress apoptosis during the course of IRI, whereas OLE combined with LY294002 up-regulated the ratio of Bax/Bcl-2 and CC3 expression, as well as the number of TUNEL-positive cells. Accordingly, we further explored whether the neuroprotective effect and anti-apoptotic mechanism of OLE was mediated by the Akt/GSK3 signaling pathway.

The serine-threonine kinase Akt, which can be directly activated by PI3K-mediated phosphorylation, can be inhibited by LY294002 [44]. Activated Akt coordinates intracellular signals and regulated several downstream targets of the cell death/survival pathways to inhibit apoptosis, including glycogen synthase kinase-3(GSK-3) [45]. Akt phosphorylation regulates cell proliferation and promotes cell survival by subsequent inactivation of GSK-3 β [20]. In the early step in the execution phase of cellular apoptosis, phosphorylated GSK-3 serves as an upstream regulator of programmed cell death to aggravate cell damage and increase caspase-3 activity, which is important in central nervous system diseases [46]. In the present study, the OLE treatment evidently elevated the expression of activated Akt (Ser473) over 5 days after IRI, which then successively decreased the expression of activated GSK-3 β (Ser9). OLE treatment can alleviate neuronal apoptosis and reduce expression of apoptotic apoptosis regulating proteins. LY294002 combined with OLE administration showed similar levels of the p-Akt/Akt and p-GSK-3 β /GSK-3 β ratio as that of the vehicle group. LY294002 plus OLE treatment could not confer anti-apoptotic effects reducing the incidence of cell apoptosis after IRI. Our results further confirm that OLE treatment exerts a neural-protective effect in a rat model of IRI by means of activation of the PI3K/Akt signaling pathway and inhibiting GSK-3 β . However, PI3K/Akt/GSK3 β may contribute to the activation of autophagy. Regulation of autophagy and several other mechanisms are all possible mechanisms underlying the decreased expression of caspase-3 and Bax, which was reported by previous studies [47,48]. Whether autophagy was involved in the neuroprotective effect exerted by OLE after IRI *in vivo* should be further explored.

The neurotrophins BDNF and NGF, which are produced and released by a variety of neuronal and non-neuronal cells, are important regulators involved in plasticity and neuron survival [49]. In the present study, we discovered that NGF and BDNF were downregulated in the vehicle group and that OLE treatment reversed this downregulation. In contrast to rats in the OLE group, the administration of LY294002 plus OLE

canceled the protective effect. A previous study has also indicated that the OLE-induced neuroprotective effect observed may be due to increased BDNF and NGF, as well as decreased level of reduced glutathione (GSH) [50].

Conclusions

We found that OLE protected against IRI and improved neurological and cognitive function by reducing apoptosis *in vivo*.

References:

1. Sahota P, Savitz SI: Investigational therapies for ischemic stroke: Neuroprotection and neurorecovery. *Neurotherapeutics*, 2011; 8(3): 434–51
2. Gursoy-Ozdemir Y, Yemisci M, Dalkara T et al: Microvascular protection is essential for successful neuroprotection in stroke. *J Neurochem*, 2012; 123: 2–11
3. Chiang KL, Cheng CY: Epidemiology, risk factors, and characteristics of pediatric stroke: A nationwide population-based study. *QJM*, 2018; 1: 10
4. Chamorro Á, Dirnagl U, Urra X et al: Neuroprotection in acute stroke: Targeting excitotoxicity, oxidative and nitrosative stress, and inflammation. *Lancet Neurol*, 2016; 15(8): 869–81
5. Szydlowska K, Tymianski M: Calcium, ischemia and excitotoxicity. *Cell Calcium*, 2010; 47(2): 122–29
6. Zhang F, Liu J, Shi JS: Anti-inflammatory activities of resveratrol in the brain: Role of resveratrol in microglial activation. *Eur J Pharmacol*, 2010; 636(1): 1–7
7. Zhang X, Zhou Y, Li H et al: Intravenous administration of DPSCs and BDNF improves neurological performance in rats with focal cerebral ischemia. *Int J Mol Med*, 2018; 41(6): 3185–94
8. Graham SH, Chen J: Programmed cell death in cerebral ischemia. *J Cereb Blood Flow Metab*, 2001; 21(2): 99–109
9. Ryan F, Khodaghohi F, Dargahi L et al: Temporal pattern and crosstalk of necroptosis markers with autophagy and apoptosis associated proteins in ischemic hippocampus. *Neurotox Res*, 2018; 34(1): 79–92
10. Nogami-Hara A, Nagao M, Takasaki K et al: The Japanese Angelica acutiloba root and yokukansan increase hippocampal acetylcholine level, prevent apoptosis and improve memory in a rat model of repeated cerebral ischemia. *J Ethnopharmacol*, 2018; 214: 190–96
11. Janahmadi Z, Nekooeian AA, Moaref AR et al: Oleuropein attenuates the progression of heart failure in rats by antioxidant and antiinflammatory effects. *Naunyn Schmiedeberg Arch Pharmacol*, 2017; 390(3): 245–52
12. Sherif IO, Nakshabandi ZM, Mohamed MA et al: Uroprotective effect of oleuropein in a rat model of hemorrhagic cystitis. *Int J Biochem Cell Biol*, 2016; 74: 12–17
13. Angeloni C, Malaguti M, Barbalace MC et al: Bioactivity of olive oil phenols in neuroprotection. *Int J Mol Sci*, 2017; 18(11): pii: E2230
14. González-Corraea JA, Muñoz-Marín J, Arrebola MM et al: Dietary virgin olive oil reduces oxidative stress and cellular damage in rat brain slices subjected to hypoxia-reoxygenation. *Lipids*, 2007; 42(10): 921–29
15. Zhao Q, Bai Y, Li C et al: Oleuropein protects cardiomyocyte against apoptosis via activating the reperfusion injury salvage kinase pathway *in vitro*. *Evid Based Complement Alternat Med*, 2017; 2017: 2109018
16. Khalatbary AR, Ahmadvand H: Neuroprotective effect of oleuropein following spinal cord injury in rats. *Neurol Res*, 2012; 34(1): 44–51
17. Romorini L, Garate X, Neiman G et al: AKT/GSK3 β signaling pathway is critically involved in human pluripotent stem cell survival. *Sci Rep*, 2016; 6: 35660
18. Endo H, Nito C, Kamada H et al: Activation of the Akt/GSK3 β signaling pathway mediates survival of vulnerable hippocampal neurons after transient global cerebral ischemia in rats. *J Cereb Blood Flow Metab*, 2006; 26(12): 1479–89
19. Yu Z, Tang L, Chen L et al: Erythropoietin reduces brain injury after intracerebral hemorrhagic stroke in rats. *Mol Med Rep*, 2013; 8(5): 1315–22
20. Zhang DD, Shi N, Fang H et al: Vildagliptin, a DPP4 inhibitor, alleviates diabetes-associated cognitive deficits by decreasing the levels of apoptosis-related proteins in the rat hippocampus. *Exp Ther Med*, 2018; 15(6): 5100–6
21. Shapira M, Licht A, Milman A et al: Role of glycogen synthase kinase-3 β in early depressive behavior induced by mild traumatic brain injury. *Mol Cell Neurosci*, 2007; 34(4): 571–77
22. Krafft PR, Altay O, Rolland WB et al: $\alpha 7$ nicotinic acetylcholine receptor agonism confers neuroprotection through GSK-3 β inhibition in a mouse model of intracerebral hemorrhage. *Stroke*, 2012; 43(3): 844–50
23. Longa EZ, Weinstein PR, Carlson S et al: Reversible middle cerebral artery occlusion without craniectomy in rats. *Stroke*, 1989; 20(1): 84–91
24. Zaidi HA, Zabramski JM, Safavi-Abbasi S et al: Spontaneous intracerebral hemorrhage. *World Neurosurg*, 2015; 84(5): 1191–92
25. Cui CM, Gao JL, Cui Y et al: Chloroquine exerts neuroprotection following traumatic brain injury via suppression of inflammation and neuronal autophagic death. *Mol Med Rep*, 2015; 12(2): 2323–28
26. Li P, Su L, Li X et al: Remote limb ischemic postconditioning protects mouse brain against cerebral ischemia/reperfusion injury via upregulating expression of Nrf2, HO-1 and NQO-1 in mice. *Int J Neurosci*, 2015; 126(6): 552–59
27. Spencer RL, Kalman BA, Cotter CS et al: Discrimination between changes in glucocorticoid receptor expression and activation in rat brain using western blot analysis. *Brain Res*, 2000; 868(2): 275–86
28. Gao C, Liu Y, Jiang Y et al: Geniposide ameliorates learning memory deficits, reduces Tau phosphorylation and decreases apoptosis via GSK3 β pathway in streptozotocin-induced alzheimer rat model. *Brain Pathol*, 2014; 24(3): 261–69
29. Lu X, Hong Z, Tan Z et al: Nicotinic acetylcholine receptor alpha7 subunit mediates vagus nerve stimulation-induced neuroprotection in acute permanent cerebral ischemia by a7nAChR/JAK2 pathway. *Med Sci Monit*, 2017; 23: 6072–81
30. Lakhan SE, Kirchgessner A, Hofer M: Inflammatory mechanisms in ischemic stroke: Therapeutic approaches. *J Transl Med*, 2009; 7(1): 97
31. Ma XD, Song JN, Zhang M et al: Advances in research of the neuroprotective mechanisms of cerebral ischemic postconditioning. *Int J Neurosci*, 2015; 125(3): 161–69
32. Visioli F, Poli A, Gall C: Antioxidant and other biological activities of phenols from olives and olive oil. *Med Res Rev*, 2002; 22(1): 65–75
33. Khalatbary AR, Ahmadvand H: Effect of oleuropein on tissue myeloperoxidase activity in experimental spinal cord trauma. *Iran Biom J*, 2011; 15(4): 164–67
34. Goldsmith CD, Bond DR, Jankowski H et al: The olive biophenols oleuropein and hydroxytyrosol selectively reduce proliferation, influence the cell cycle, and induce apoptosis in pancreatic cancer cells. *Int J Mol Sci*, 2018; 19(7): piiE1937
35. Mohagheghi F, Bigdeli MR, Rasoulian B et al: Dietary virgin olive oil reduces blood brain barrier permeability, brain edema, and brain injury in rats subjected to ischemia-reperfusion. *ScientificWorldJournal*, 2010; 10: 1180–91
36. Efentakis P, Iliodromitis E K, Mikros E, et al. Effects of the olive tree leaf constituents on myocardial oxidative damage and atherosclerosis. *Planta Medica*, 2015; 81(08): 648–54
37. Impellizzeri D, Esposito E, Mazzon E et al: The effects of a polyphenol present in olive oil, oleuropein aglycone, in an experimental model of spinal cord injury in mice. *Biochem Pharmacol*, 2012; 83(10): 1413–26

Conflict of interest

None.

38. Zamani M, Hassanshahi J, Soleimani M et al: Neuroprotective effect of olive oil in the hippocampus CA1 neurons following ischemia: Reperfusion in mice. *J Neurosci Rural Pract*, 2013; 4(2): 164–70
39. Luo T, Liu G, Ma H et al: Inhibition of autophagy via activation of PI3K/Akt pathway contributes to the protection of ginsenoside Rb1 against neuronal death caused by ischemic insults. *Int J Mol Sci*, 2014; 15(9): 15426–42
40. Cory S, Adams JM: The Bcl2 family: Regulators of the cellular life-or-death switch. *Nat Rev Cancer*, 2002; 2(9): 647–56
41. Li Z, Zheng X, Li P et al: Effects of acupuncture on mRNA levels of apoptotic factors in perihematomal brain tissue during the acute phase of cerebral hemorrhage. *Med Sci Monit*, 2017; 23: 1522–32
42. Hu Q, Peng J, Liu W et al: Elevated cleaved caspase-3 is associated with shortened overall survival in several cancer types. *Int J Clin Exp Pathol*, 2014; 7(8): 5057–70
43. Yu H, Liu P, Tang H et al: Oleuropein, a natural extract from plants, offers neuroprotection in focal cerebral ischemia/reperfusion injury in mice. *Eur J Pharmacol*, 2016; 775: 113–19
44. Li H, Tang Z, Chu P et al: Neuroprotective effect of phosphocreatine on oxidative stress and mitochondrial dysfunction induced apoptosis *in vitro* and *in vivo*: Involvement of dual PI3K/Akt and Nrf2/HO-1 pathways. *Free Radic Biol Med*, 2018; 120: 228–38
45. Garwood ER, Kumar AS, Baehner FL et al: Fluvastatin reduces proliferation and increases apoptosis in women with high grade breast cancer. *Breast Cancer Res Treat*, 2010; 119(1): 137–44
46. Hu S, Begum AN, Jones MR et al: GSK3 inhibitors show benefits in an Alzheimer's disease (AD) model of neurodegeneration but adverse effects in control animals. *Neurobiol Dis*, 2009; 33(2): 193–206
47. Feng FB, Qiu HY: Effects of Artesunate on chondrocyte proliferation, apoptosis and autophagy through the PI3K/AKT/mTOR signaling pathway in rat models with rheumatoid arthritis. *Biomed Pharmacother*, 2018; 102: 1209–20
48. Maiuri MC, Zalckvar E, Kimchi A et al: Self-eating and self-killing: Crosstalk between autophagy and apoptosis. *Nat Rev Mol Cell Biol*, 2007; 8(9): 741–52
49. Li R, Ma JF, Wu YQ et al: Dual delivery of NGF and bFGF coacervate ameliorates diabetic peripheral neuropathy via inhibiting schwann cells apoptosis. *Int J Biol Sci*, 2017; 13(5): 640–51
50. Carito V, Venditti A, Bianco A et al: Effects of olive leaf polyphenols on male mouse brain NGF, BDNF and their receptors TrkA, TrkB and p75. *Nat Prod Res*, 2014; 28(22): 1970–84.